Vertical stabilization of ITER plasma using explicit model predictive control

Samo Gerkšič[a], Gianmaria de Tommasi[b]

[a] *Jožef Stefan Institute, Jamova 39, Ljubljana, Slovenia*
[b] *Associazione EURATOM-ENEA-CREATE, Univ. di Napoli Federico II, Via Claudio 21, 80125, Napoli, Italy*

In this work we explore advanced control algorithms for the vertical stabilization of plasma in the ITER tokamak for the case where a combination of ohmic in-vessel and superconducting poloidal actuators is used for effective response to disturbances subject to thermal constraints. We apply constrained linear-quadratic optimal control, which is a hybrid between conventional linear quadratic optimal control and model predictive control (MPC). We discuss the issues of practical implementation in the form of explicit MPC, which allows application to fast processes by avoiding the use of on-line optimization.

Keywords: tokamak control, vertical stabilization system, optimal control, constrained linear quadratic control, explicit model predictive control.

1. Introduction

Recent developments in vertical control of unstable elongated plasma in tokamak fusion reactors are focused on the ability to withstand large-scale disturbances, such as vertical displacement events (VDE) and edge localized mode (ELM) perturbations [1,2]. One of the design proposals for the ITER tokamak [3] provides the implementation of plasma vertical stabilization (VS) system by using a combination of actuators: ohmic in-vessel (IV) coils, in order to assure a prompt and effective response to the envisaged disturbances, and superconducting (SC) poloidal field coils, to meet the thermal constraints that must be fulfilled for the IV coils.

Constrained linear quadratic (CLQ) optimal control is a systematic approach to control of systems involving constraints. It is a hybrid of LQ control and model predictive control (MPC). CLQ increases the convergence region of initial states compared to LQ control, so it should allow rejection of larger VDE/ELM perturbations if it is adopted for the VS system.

Conventional implementations of CLQ/MPC using on-line optimization are computationally infeasible for fast control loops such as the ITER VS system. However, explicit CLQ/MPC [4] shifts the bulk of computation out of the real-time control loop. It produces a piecewise-affine control law defined over a finite polyhedral partition of the system state-space. In real-time, the controller requires the evaluations of a few linear inequalities and of the local affine control law.

In this work we apply CLQ control to the ITER tokamak model. The practical application of CLQ to systems with multiple inputs and outputs is not straightforward; some of the issues have been recently described in [5]. The control problem setup needs to be simplified in order to achieve a tractable and numerically reliable off-line computation. The complications arise from the practical requirements for a relatively short sampling time, needed for fast controller response, and a relatively long constraint-handling horizon, needed for timely reactions to anticipated activity of constraints. We start with a brief overview of CLQ/MPC; then we present the simulation setup, and the implementation and results of LQ, CLQ and MPC controllers.

2. MPC and CLQ control setup

Consider the discrete-time state-space system

$$\mathbf{x}(k+1) = \mathbf{A}\mathbf{x}(k) + \mathbf{B}\mathbf{u}(k),\ \ \mathbf{y}(k) = \mathbf{C}\mathbf{x}(k) \quad (1)$$

with system matrices **A**, **B**, **C**, input **u**, output **y**, state **x**, and time index *k*, and the problem of its regulation to the origin, fulfilling the signal constraints $\mathbf{u}_{\min} \le \mathbf{u} \le \mathbf{u}_{\max}$, $\mathbf{y}_{\min} \le \mathbf{y} \le \mathbf{y}_{\max}$ and minimising the cost function

$$J = \sum_{j=0}^{N-1} (\mathbf{x}_{k+j|k}^T \mathbf{Q}_x \mathbf{x}_{k+j|k} + \mathbf{u}_{k+j|k}^T \mathbf{R}_u \mathbf{u}_{k+j|k}) + \\ + \mathbf{x}_{k+N|k}^T \mathbf{P}_N \mathbf{x}_{k+N|k} \quad (2)$$

with horizon *N*, cost matrices $\mathbf{Q}_x, \mathbf{R}_u$, and terminal cost $\mathbf{P}_N$ [4,6]. The LQ problem assumes $N = \infty$ with no $\mathbf{P}_N$, and finds the solution in the form of state-feedback $\mathbf{u} = \mathbf{K}_{LQ}\mathbf{x}$ by solving the associated Riccati equation, ignoring the constraints. Traditional MPC solves the constrained problem with a finite *N* by reformulation into an optimization problem which is, assuming standard control signal parameterization, solved with respect to a finite number of future control outputs $\tilde{\mathbf{u}} = [\mathbf{u}_k, ..., \mathbf{u}_{k+N-1}]$ as optimization variables.

In CLQ, the infinite-horizon constrained optimum is found by using a dual-mode controller which appends a terminal LQ controller at the end of a finite-*N* MPC problem, assuming that the constraints are not violated at $k \ge N$. The appending is carried out by

- using the solution of the associated Riccati equation $\mathbf{P}_{LQ}$ as $\mathbf{P}_N$,

author's email: samo.gerksic@ijs.si

- enforcing the LQ invariant set X_{LQ}, in which the LQ solution is feasible with respect to the signal constraints, as a terminal constraint $\mathbf{x}_{k+N|k} \in X_{LQ}$.

With the "feedback" control signal parameterization, MPC optimizes deviations $\tilde{\mathbf{f}} = [\mathbf{f}_k, ..., \mathbf{f}_{k+N-1}]$ from the LQ feedback law, $\mathbf{u} = \mathbf{K}_{LQ}\mathbf{x} + \mathbf{f}$, rather than $\tilde{\mathbf{u}}$ directly.

3. Vertical control of ITER plasma

3.1 Simulation model

Both the simulations and the controller design presented in this paper are based on high-order CREATE-L and CREATE-NL linearized dynamical models of the plasma and the surrounding coils [7,8]. The plasma linear model 1 for the equilibrium at plasma current $I_p = 14.5\,\text{MA}$, poloidal beta $\beta_p = 0.11$ and internal inductance $l_i = 0.85$ has been considered as nominal model, while the substantially different plasma model 2 for the equilibrium at $I_p = 15\,\text{MA}$, $\beta_p = 0.1$ and $l_i = 1.21$ was used for a preliminary robustness verification.

For vertical control, a two-input two-output subsystem was considered, where the inputs are

- the voltage applied to the IV coils VS3 $u_1 = u_{ic}$
- the voltage applied to the SC circuit VS1 $u_2 = u_{VS1}$

while the controlled outputs are

- the current in the IV coils $y_1 = x_{ic}$
- the plasma vertical velocity $y_2 = v_p$

Simulations also show plasma position z_p and the current in the superconductive VS1 circuit i_{VS1}.

In typical performance tests, a 10cm VDE event was simulated with a suitable initial state of the plasma linear model. Additionally, ELM disturbances may be simulated by injecting recorded profiles of β_p and l_i [3]. As performance measures, root-integral-square-error (RISE) values of x_{ic} (in-vessel coil thermal load) and v_p (vertical velocity regulation efficiency) were observed.

3.2 Static output feedback (SOF) control scheme

For reference, the results are compared with the SOF controller of Ambrosino et al. [3,9]

$$\mathbf{u}(t) = \mathbf{K}\mathbf{y}(t), \quad \mathbf{K} = \begin{bmatrix} 0.00285 & -2309 \\ 0.2 & 0 \end{bmatrix} \quad (3)$$

which provides relatively efficient and robust performance despite its simple implementation.

3.3 LQ control

A continuous-time (ct) linear-quadratic-Gaussian (LQG) optimal control scheme in Fig. 1 was the first intermediate control design step. A low-order approximation of the subsystem comprising the power supply models, the relevant part of the plasma model, and the diagnostics model, was sought. Low-order models are needed for explicit MPC (eMPC) and to avoid "over-fitting" considering the huge range of dynamics that the controller is expected to cope with. A third-order model $\{\mathbf{A}_r, \mathbf{B}_r, \mathbf{C}_r, \mathbf{0}\}$ obtained using Schur balanced truncation [10] was selected for LQG design. Model states are not measured, so a Kalman filter (KF) is used for state estimation. A saturation block prevents controller windup in case of unenforceable control signals.

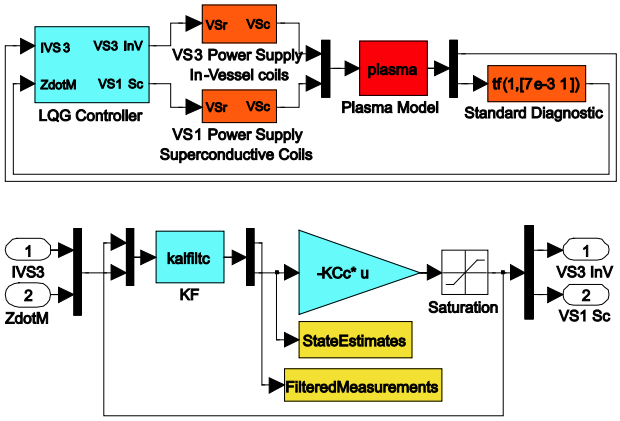

Fig. 1 LQG control scheme (top) and LQG controller block expanded (bottom).

The LQG scheme may be sensitive to modeling error, which may be addressed using the concepts of Loop Transfer Recovery [11]. Tuning is challenging because of the large number of parameters; it was carried out using a graphical tuning environment for linear closed-loop analysis based on Nyquist and Nichols diagrams with both plasma models. The following parameters were chosen for the ctLQ controller and the KF

$$\mathbf{Q}_{\mathbf{y}} = \begin{bmatrix} 0.00001 & 0 \\ 0 & 1 \end{bmatrix}, \quad \mathbf{R}_{\mathbf{u}} = \begin{bmatrix} 0.008 & 0 \\ 0 & 0.0001 \end{bmatrix} \quad (4)$$

$$\mathbf{Q}_{KF,\mathbf{y}} = \mathbf{B}_r\mathbf{B}_r^T, \quad \mathbf{R}_{KF,\mathbf{u}} = \begin{bmatrix} 0.001 & 0 \\ 0 & 10^{-13} \end{bmatrix} \quad (5)$$

Compared to the original SOF controller, the ctLQG slightly improves the performance (less thermal load on the IV coils and less v_p overshoot, see Table 1 and Fig. 4) and the robustness (better stability margins and performance with model 2). The improvement is mainly due to the faster response of u_2, which is controlled directly from y_2 instead of from delayed y_1.

The following step is a discrete-time implementation of the LQG scheme (dtLQ). Discretization of the reduced-order model using the zero-order hold approach is used, with the sampling time $T_s = 0.005\,\text{s}$; the same cost matrices are used. Compared to ctLQ, dtLQ exhibits a noticeable deterioration of performance and robustness (no longer stabilizes model 2 with the same tuning). However, a shorter sampling time has adverse impact on explicit CLQ/MPC implementation.

In Fig. 4, u_2 is clipped at the start of ctLQ and dtLQ simulations, therefore the response is not optimal.

3.4 CLQ controller

A CLQ controller is expected to provide optimal response with respect to the cost function (2) and constraints on control signals, with stability and feasibility guaranteed in the domain of attraction corresponding to the whole controller partition [12, 6]. So one may attempt to reduce the v_p overshoot observed in Fig. 4 by specifying constraints

$$\begin{bmatrix} -1.5\cdot 10^3 & -6\cdot 10^3 \end{bmatrix}^T \le \mathbf{u} \le \begin{bmatrix} 1.5\cdot 10^3 & 6\cdot 10^3 \end{bmatrix}^T$$
$$\begin{bmatrix} -5\cdot 10^4 & -5 \end{bmatrix}^T \le \mathbf{y} \le \begin{bmatrix} 2\cdot 10^4 & 5 \end{bmatrix}^T \qquad (6)$$

The construction of the CLQ controller is based on the same model as dtLQ. The same cost matrices (4) are converted to an equivalent state-cost formulation. dtLQ is applied as the terminal LQ law, using feedback parameterization. Fig. 2 shows firstly the LQ invariant set X_{LQ} in which no constraints are violated and the dtLQ solution is already optimal subject to constraints (6), then the state partition of the CLQ with the horizon N = 2, illustrating how much this CLQ increases the feasible region. The partition is the union of polyhedral regions of the controller, which are characterized by the same set of active constraints and the same local affine control law; it is computed using the Multi-Parametric Toolbox (MPT) [12] with modifications [13]. The CLQ controller is used in a scheme similar to LQG in Fig. 1, with the LQ gain replaced by the eMPC controller block.

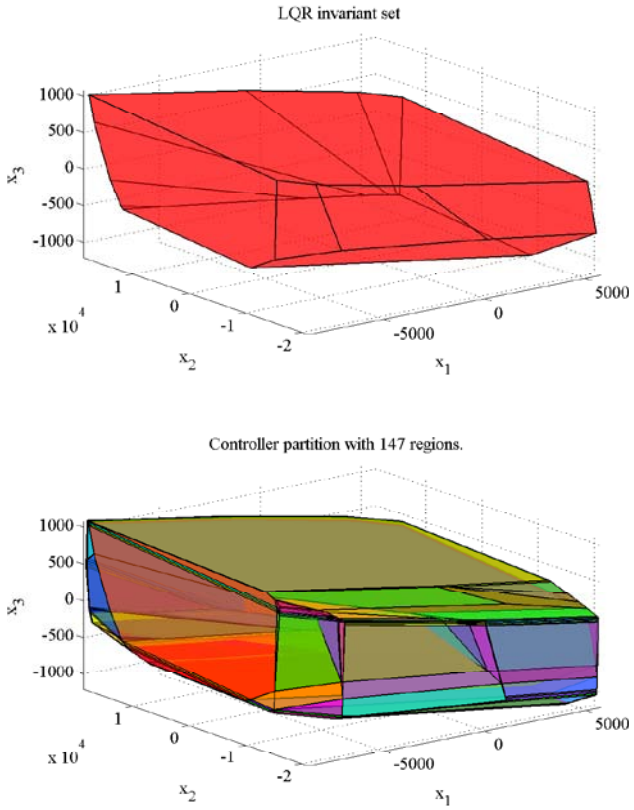

Fig. 2 The invariant set of the terminal LQ controller (top) and the CLQ controller partition (bottom).

Unfortunately, this attempt of reducing the v_p overshoot fails due to a number of practical issues, and several assumptions required for the favorable theoretical properties to hold are violated:

- Due to numerical issues, the horizon N = 2 achievable in the explicit implementation is very short. This is much shorter than the initial u_2 saturation in Fig. 4, and the CLQ controller is infeasible in the corresponding states [14].
- With such short horizon, the controller is incapable of a timely reaction to an approaching violation of output constraints.
- The online implementation of the same controller is possible with longer horizons. However, with the terminal LQ set constraint the problem remains infeasible. The feasible partition space does generally grow with increasing N, but only at some of its facets. If the terminal LQ set constraint is dropped, the feasible partition space increases, however the trajectory is not optimal and is likely to run into infeasible space.
- Underestimation of v_p in open-loop prediction due to model inaccuracy is another observed cause of running into infeasibility.

3.5 A practical eMPC controller

A practically useful and computationally tractable eMPC controller that avoids infeasibility and achieves a reduction of the v_p overshoot may be reached by departures from the theoretical CLQ setup:

- Control move blocking reduces the number of decision variables and improves numerical conditioning.
- Soft **y** constraints, which replace hard inequality constraints on predicted signal values with an additional term in the cost function penalizing constraint violations, are used to avoid infeasibility problems, but they are challenging computationally due to the additional decision variables. Softening of **y** constraints may be used when combined with sparse placement of **y** constraints over the horizon.

The eMPC controller was implemented using the Yalmip [15] method of MPT [12] with modifications [13]. It is based on the same model as dtLQ, with cost matrices (2) converted to an equivalent state-cost formulation. It uses the conventional control signal parameterization, horizon N = 9 with move blocking of **u** into two groups with 2 and 7 elements, respectively; LQ terminal cost with no terminal constraint; tighter soft output constraints $[-5\cdot 10^4 \quad -5]^T \le \mathbf{y} \le [1.8\cdot 10^4 \quad 5]^T$; and soft constraint cost $\mathbf{S}_\mathbf{y} = 10^{-4}\cdot \mathbf{I}_2$ (where $\mathbf{I}_2$ is the identity matrix of dimension 2). The partition of the basic version of eMPC with **y** constraints at each horizon sample in the top section of Fig. 3 contains 4826 regions; eMPC-SC2 with **y** constraints at each second sample 1462 regions; eMPC-SC4 with **y** constraints at each fourth sample in the bottom section of Fig. 3 531 regions, respectively. Thus, Fig. 3 visually displays the reduction in the density of partitioning of the feasible state-space. A considerable simplification of the controller partition is achieved; however it is accompanied by a deterioration of the performance as seen in Table 1 and Fig. 4. With soft **y** constraints, the partitions in Fig. 3 are much larger than

the one in the bottom part of Fig. 2, as the controller does not become infeasible if an output constraint is violated.

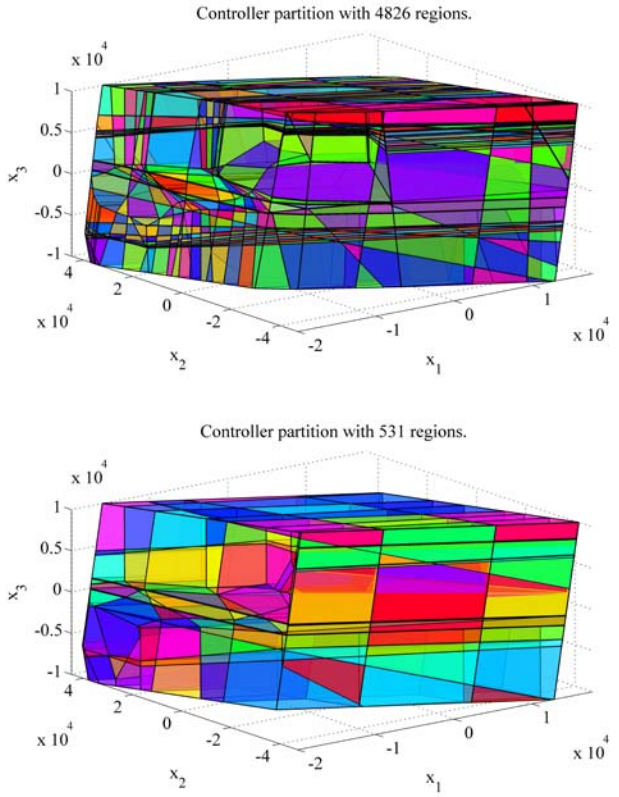

Fig. 3 EMPC controller partition: output constraints at each sample (top) and eMPC-SC4 (bottom).

Table 1: Controller performance

Controller	In-vessel coil thermal load $\mathrm{RISE}(x_{ic}(t))$	Vertical velocity regulation $\mathrm{RISE}(v_p(t))$
SOF	9805.7	0.10786
ctLQ	8239.4	0.09625
dtLQ	8563.6	0.11658
eMPC	8061.0	0.11097
eMPC-SC4	8291.3	0.11136

4. Conclusions

A computationally tractable explicit MPC controller for the plasma VS system capable of practically useful constraint-handling was demonstrated. Softening of the output constraints was required for feasibility, while computational tractability was reached by using move blocking and sparse placement of constraints.

Acknowledgments

This work was supported in part by the Republic of Slovenia, Ministry of Education, Science, Culture and Sport and European Union (EU) - European Regional Development Fund (Competence Centre for Advanced Control Technologies) and by the Slovenian Research Agency (L2-2342).

References

[1] A. Neto et al., Exploitation of Modularity in the JET Tokamak VS System, Control Eng. Pract. **20**, 9 (2012)

[2] T. Bellizio et al., Control of elongated plasma in presence of ELMs in the JET tokamak, IEEE T. Nucl. Sci. **58**, 4 (2011)

[3] G. Ambrosino et al., Plasma Vertical Stabilization in the ITER Tokamak via Constrained Static Output Feedback, IEEE T. Contr. Syst. T. **19**, 2 (2011)

[4] A. Bemporad et al., The explicit LQ regulator for constrained systems, Automatica **38**, 1 (2002)

[5] P. Patrinos and H. Sarimveis, A new algorithm for solving convex parametric quadratic programs based ongraphical derivatives of solution mappings, Automatica **46,** 9 (2010)

[6] D.Q. Mayne et al., Constrained model predictive control: Stability and optimality, Automatica **36**, 6 (2000)

[7] R. Albanese and F. Villone, The linearized CREATE-L plasma response model for the control of current, position and shape in tokamaks, Nucl. Fus. **38**, 5 (1998)

[8] R. Albanese et al., Plasma response models for current, shape and position control at JET, Fusion Eng. Des. **66–68** (2003)

[9] G. Ambrosino et al., Robust vertical control of ITER plasmas via static output feedback, Proc. IEEE MSC'11, Denver CO (2011)

[10] M. G. Safonov and R. Y. Chiang, A Schur Method for Balanced Model Reduction, IEEE T. Automat. Contr. **34**, 7, (1989)

[11] J.M. Maciejowski, Multivariable Feedback Design (Addison-Wesley, Wokingham UK, 1989)

[12] M. Kvasnica et al., Multi-parametric toolbox, version 2.6.2 (2004) [Online: http://control.ee.ethz.ch/mpt/]

[13] S. Gerkšič, Improving reliability of partition computation in explicit MPC with MPT Toolbox, Proc. 18th IFAC WC, Milano IT (2011)

[14] P. Grieder et al., Computation of the constrained infinite time linear quadratic regulator, Automatica **40**, 4 (2004)

[15] J. Löfberg, YALMIP: A Toolbox for Modeling and Optimization in MATLAB. Proc. CACSD Conference, Taipei (2004)

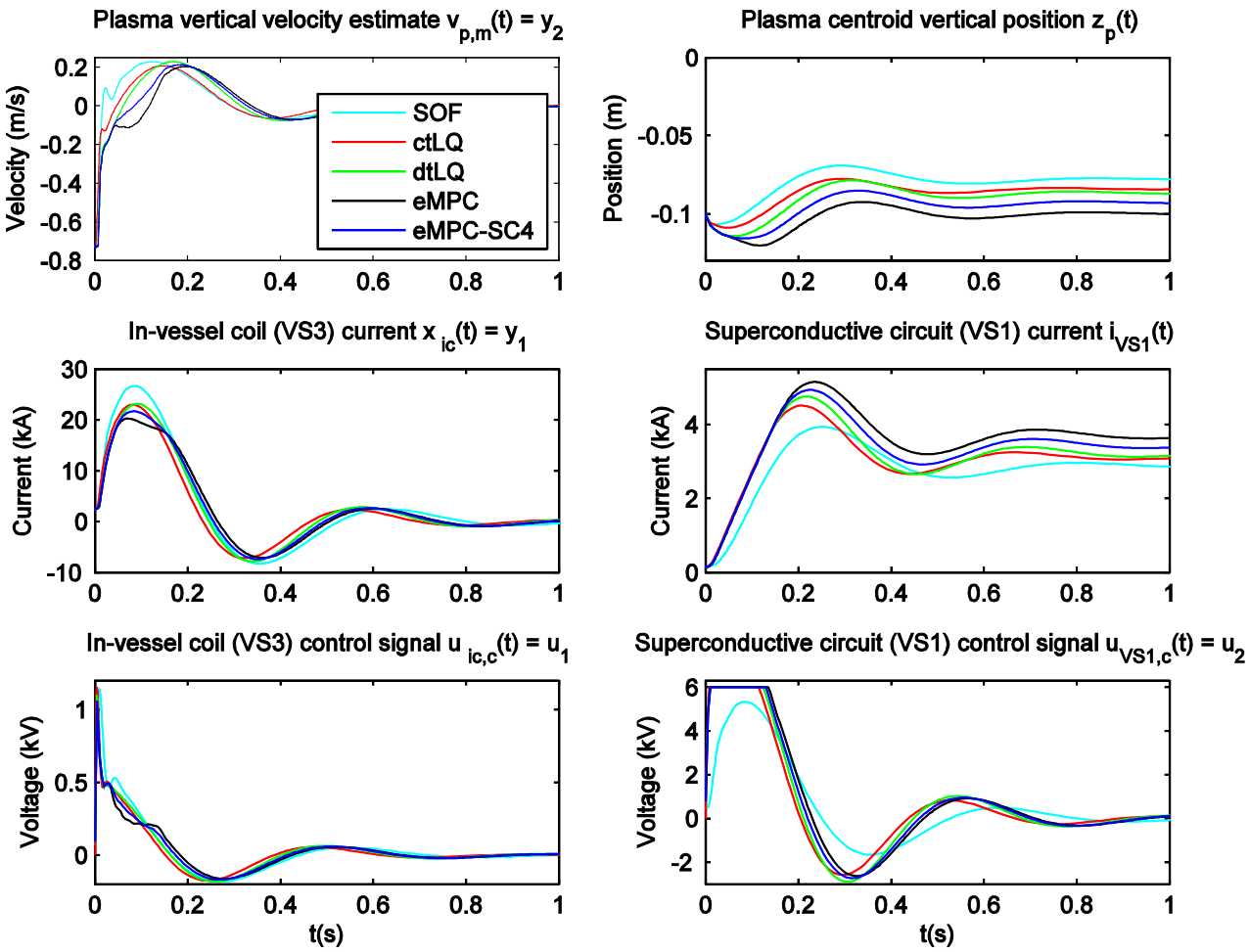

Fig. 4 Closed-loop response to a 10 cm VDE, model 1.